N-terminus GTPase domain of the cytoskeleton protein FtsZ plays a critical role in its adaptation to high hydrostatic pressure

Xue-Hua Cui[1,2], Yu-Chen Wei[1], Xue-Gong Li[1,3], Xiao-Qing Qi[1,3†], Long-Fei Wu[1,3,4] and Wei-Jia Zhang[1,3]*

[1]Laboratory of Deep-Sea Microbial Cell Biology, Institute of Deep-Sea Science and Engineering, Chinese Academy of Sciences, Sanya, China, [2]College of Earth and Planetary Sciences, University of Chinese Academy of Sciences, Beijing, China, [3]Institution of Deep-Sea Life Sciences, IDSSE-BGI, Sanya, China, [4]Aix Marseille University, CNRS, LCB, Marseille, France

Studies in model microorganisms showed that cell division is highly vulnerable to high hydrostatic pressure (HHP). Disassembly of FtsZ filaments induced by HHP results in the failure of cell division and formation of filamentous cells in *E. coli*. The specific characteristics of FtsZ that allow for functional cell division in the deep-sea environments, especially in obligate piezophiles that grow exclusively under HHP condition, remain enigmatic. In this study, by using a self-developed HHP *in-situ* fixation apparatus, we investigated the effect of HHP on FtsZ by examining the subcellular localization of GFP-tagged FtsZ *in vivo* and the stability of FtsZ filament *in vitro*. We compared the pressure tolerance of FtsZ proteins from pressure-sensitive strain *Shewanella oneidensis* MR-1 (FtsZ$_{So}$) and obligately piezophilic strain *Shewanella benthica* DB21MT-2 (FtsZ$_{Sb}$). Our findings showed that, unlike FtsZ$_{So}$, HHP hardly affected the Z-ring formation of FtsZ$_{Sb}$, and filaments composed of FtsZ$_{Sb}$ were more stable after incubation under 50 MPa. By constructing chimeric and single amino acid mutated FtsZ proteins, we identified five residues in the N-terminal GTPase domain of FtsZ$_{Sb}$ whose mutation would impair the Z-ring formation under HHP conditions. Overall, these results demonstrate that FtsZ from the obligately piezophilic strain exhibits superior pressure tolerance than its homologue from shallow water species, both *in vivo* and *in vitro*. Differences in pressure tolerance of FtsZ are largely attributed to the N-terminal GTPase domain. This represents the first in-depth study of the adaptation of microbial cytoskeleton protein FtsZ to high hydrostatic pressure, which may provide insights into understanding the complex bioprocess of cell division under extreme environments.

KEYWORDS

obligate piezophile, cell division, cytoskeleton, FtsZ, high hydrostatic pressure, GTPase domain

1 Introduction

Bacterial division is initiated with Z-ring formation. The cytoskeletal protein FtsZ assembles into a ring-like structure named Z ring at the septum of a dividing cell and serves as a scaffold for the assembly of the divisome (Adams and Errington, 2009). FtsZ is a prokaryotic homologue of tubulin. It consists of an N-terminal tubulin-like core domain that contains GTP binding residues, an intrinsically disordered C-terminal linker region possibly involved in modulating lateral interactions, and a highly conserved short peptide at its C-terminus that interacts with accessory proteins such as FtsA and ZipA, and tethers FtsZ filament to the membrane (Ma and Margolin, 1999; Stricker and Erickson, 2003; Redick et al., 2005; Buske and Levin, 2012, 2013; Gardner et al., 2013; Arjes et al., 2015; Sundararajan and Goley, 2017).

Structural studies suggested that FtsZ are present in open and closed conformations, and switch from closed conformation to open conformation during FtsZ polymerization process. FtsZ polymerizes in a head-to-tail manner, and at the inter-subunit interface forms the catalytic site for GTP hydrolysis. The free FtsZ subunits in closed conformation are prone to assembly into a filament and the hydrolysis of GTP produces GDP-bound FtsZ subunits that are weakened in longitudinal bonds and are prone to disassociate from the other end of the filament (Mukherjee and Lutkenhaus, 1994; Mukherjee, 1998; Redick et al., 2005; Jindal and Panda, 2013; Arjes et al., 2015; Wagstaff et al., 2017). The dynamic treadmilling of FtsZ filaments enables the movement of divisiomes and the even distribution of newly synthesized septal peptidoglycan along the division ring. Mutations of FtsZ with reduced GTPase activity may stabilize the polymer *in vitro* and *in vivo*, and result in a lower rate of treadmilling, an altered septum and peptidoglycan structure, and consequently abnormal cell division (Lu et al., 2001; Stricker et al., 2002; Bisson-Filho et al., 2017; Yang et al., 2017; Monteiro et al., 2018; Perez et al., 2019).

Despite an essential bioprocess, cell division is highly vulnerable to high hydrostatic pressures (HHP). Simulation studies showed that HHP of 30 MPa induced spherical or spindle-shaped epithelial cells, and cell division of *Escherichia coli* was inhibited at 50 MPa and formed filamentous cells (Bourns et al., 1988; Ishii et al., 2004). In these elongated cells, the expression of FtsZ was unaffected, but both Z-ring formation and nucleoids partition were impaired. In addition, the filament of purified FtsZ dissociated *in vitro* as a function of increased pressure. A hypothesis was thus proposed that the failure of FtsZ polymerization and Z-ring formation restrained division of *E.coli* cells under high pressures (Ishii et al., 2004; Kawarai et al., 2004; Aertsen and Michiels, 2005). Similar phenomenon has been observed in eukaryotes. Elevated pressure induced rapid and reversible depolymerization of microtubules in diverse eukaryotic cells (Messier and Seguin, 1978; Arai et al., 2008). *In vitro* studies showed that the application of HHP led to depolymerization of microtubules from both ends, suggesting a decrease of intermolecular interactions between tubulin molecules (Bravim et al., 2010; Hayashi et al., 2016; Takiguchi et al., 2018).

Inhabiting the deep oceanic areas are microbes acclimated to high pressures. They grow preferably (termed as piezophiles) or exclusively (obligate piezophiles) at elevated pressure conditions. To cope with high pressures, deep-sea microbes developed metabolic pathways with higher pressure tolerance, regulation systems responsive to changes in pressure, and cellular membranes with increased proportion of unsaturated fatty acids (Li et al., 1998; Allen et al., 1999; Xiao et al., 2021; Allen and Bartlett, 2022; Tamby et al., 2023). However, the understanding of cell division in deep-sea piezophiles is highly inadequate. Ishii et al. first demonstrated that localization of FtsZ at the septum and the transcription of *ftsZ* in deep-sea strain *Shewanella violacea* DSS12 was not affected by increasing of pressure (Ishii et al., 2002). Kawamoto et al. further showed that despite the presence of Z-rings, deficient of eicosapentaenoic acid (EPA) may lead to defects of cell division and elongated cells under high pressure conditions, suggesting polyunsaturated fatty acid played an important role in the late stage of division under high pressure condition (Kawamoto et al., 2011). Recently we found that HHP impaired the cell division of strain *Tepidibacter hydrothermalis* SWIR-1 isolated from deep-sea hydrothermal vent, while infrared irradiation triggered septum formation and restored cell division through an unknown mechanism (Dai et al., 2024). Collectively, the cellular division under HHP is a complex process affected by many factors, and how is the functional Z-ring formed under high pressure conditions remain unknown. In this study, we analyzed the effect of HHP on FtsZ from pressure sensitive *Shewanella oneidensis* MR-1 (FtsZ$_{So}$) in comparison with FtsZ from hadal obligately piezophilic strain *S. benthica* DB21MT-2 whose optimum growth pressure is 80 MPa (FtsZ$_{Sb}$) (Kato et al., 1998). Comparisons were performed regarding their stability under high pressures *in vivo* and *in vitro*. Furthermore, the amino acids important for the HHP adaptation of FtsZ protein were identified through analyses of chimeric proteins and mutated FtsZ$_{Sb}$ proteins.

2 Materials and methods

2.1 Strains, plasmids and growth conditions

Strains and plasmids used in this study are listed in Table 1. Strains carrying pDSW plasmids were grown at 37°C in LB medium with ampicillin at 25 μg/mL in liquid cultures and 100 μg/mL in solid cultures. Strains carrying pET plasmids were grown at 37°C in LB medium with 50 μg/mL kanamycin.

2.2 Plasmid construction

The DNA fragments of *ftsZ$_{So}$* and *ftsZ$_{Sb}$* without stop codon were amplified from chromosomal DNA of *S. oneidensis* MR-1 and *S. benthica* DB21MT-2, respectively. The *gfp* fragment was amplified from pDSW230 and fused to the 3′ end of *ftsZ$_{So}$* and *ftsZ$_{Sb}$* by over-lap PCR. The generated fragment containing *ftsZ$_{So}$-gfp* or *ftsZ$_{Sb}$-gfp* were then cloned into the pDSW230 by replacing the *ftsZ$_{Ec}$-gfp* between the XhoI and HindIII sites. Partial fragments of *ftsZ$_{So}$* and *ftsZ$_{Sb}$* were amplified from pDSW2302 and pDSW2304, respectively. By multiple steps of over-lap PCR, the fragments were assembled as follows: *ftsZ$_{So-N}$* contains nucleotides 1–954 from *ftsZ$_{So}$* and nucleotides 955–1,164 from *ftsZ$_{Sb}$*; *ftsZ$_{So-L}$* contains nucleotides 1–954 and 1,120–1,164 from *ftsZ$_{Sb}$* and nucleotides 955–1,140 from *ftsZ$_{So}$*; *ftsZ$_{So-C}$* contains nucleotides 1–1,119 from *ftsZ$_{Sb}$* and nucleotides 1141-1185 from *ftsZ$_{So}$*. The single-amino-acid mutated *ftsZ$_{Sb}$* genes were synthesized by Suzhou Jinweizhi Biotechnology Co., Ltd. The S7T replaces G20 by C, T9S replaces A25 by T, S54G carries GG at position 160 and

TABLE 1 Strains and plasmids used in this study.

Strains and plasmids	Descriptions	Source or reference
Strains		
DH5a	F⁻ φ80$lacZ$ΔM15 Δ($lacZYA$-argF)U169 recA1 endA1 hsdR17(r_K^-, m_K^+) $phoA$ supE44 λ⁻ thi-1 gyrA96 relA1	Laboratory collection
EC309	EC251 $ftsZ84$(Ts) leu::Tn10	Michael Tarry et al.
Rosetta™ (DE3)	F-ompT $hsdS_B$(r_B^- m_B^-) gal dcm (DE3) pRARE	Laboratory collection
Plasmids		
pDSW230	pDSW-FtsZ$_{Ec}$-GFP	David S. Weiss et al.
pDSW2302	pDSW-FtsZ$_{Sb}$-GFP	This study
pDSW2304	pDSW-FtsZ$_{So}$-GFP	This study
pDSW2315	pDSW-FtsZ$_{So-N}$ (FtsZ$_{So}$ 1–316 - FtsZ$_{Sb}$ 317–388)-GFP	This study
pDSW2316	pDSW-FtsZ$_{So-C}$ (FtsZ$_{Sb}$ 1–372 - FtsZ$_{So}$ 380–395)-GFP	This study
pDSW2319	pDSW-FtsZ$_{So-L}$ (FtsZ$_{Sb}$ 1–316 - FtsZ$_{So}$ 317–379 - FtsZ$_{Sb}$ 380–395)-GFP	This study
pDSW2302-1	pDSW-FtsZ$_{Sb}$ S7T-GFP	This study
pDSW2302-2	pDSW-FtsZ$_{Sb}$ T9S-GFP	This study
pDSW2302-3	pDSW-FtsZ$_{Sb}$ S54G-GFP	This study
pDSW2302-4	pDSW-FtsZ$_{Sb}$ T57S-GFP	This study
pDSW2302-5	pDSW-FtsZ$_{Sb}$ I65V-GFP	This study
pDSW2302-6	pDSW-FtsZ$_{Sb}$ I77V-GFP	This study
pDSW2302-7	pDSW-FtsZ$_{Sb}$ L80A-GFP	This study
pDSW2302-8	pDSW-FtsZ$_{Sb}$ D91A-GFP	This study
pDSW2302-9	pDSW-FtsZ$_{Sb}$ E119Q-GFP	This study
pDSW2302-10	pDSW-FtsZ$_{Sb}$ K122R-GFP	This study
pDSW2302-11	pDSW-FtsZ$_{Sb}$ R141K-GFP	This study
pDSW2302-12	pDSW-FtsZ$_{Sb}$ E152A-GFP	This study
pDSW2302-13	pDSW-FtsZ$_{Sb}$ S232R-GFP	This study
pDSW2302-14	pDSW-FtsZ$_{Sb}$ G305D-GFP	This study

161 instead of TC, T57S replaces A169 by T, I65V replaces A193 by G, I77V carries GTG at position 229–231 instead of ATA, L80A carries GC at position 238 and 239 instead of TT, D91A carries CG at position 272 and 273 instead of AT, E119Q replaces G355 by C, K122R replaces A365 by G, R141K replaces G422 by A, E152A replaces A455 by C, S232R replaces A694 by C, and G305D replaces G914 by A. The chimeric and mutated $ftsZ$ genes were fused with gfp by over-lap PCR and cloned into pDSW230 by replacing the $ftsZ_{Ec}$-gfp between the XhoI and HindIII sites. The $ftsZ_{So}$ and $ftsZ_{Sb}$ were amplified and cloned into pET28a (+) at BamHI/XhoI sites and generated His-tag at N-terminal.

2.3 Western blot analysis

The $E. coli$ strains carrying pDSW plasmids were first grown in LB medium at 37°C, atmospheric pressure, for 5 h with shaking. Then the cultures were transferred into sterilized syringes and incubated under atmospheric (0.1 MPa) and high (50 MPa) pressures for 5 h. The syringes were placed in high-pressure vessels (Feiyu Science and Technology Exploitation Co., Ltd., Nantong, China), and the hydrostatic pressure was applied with a water pump (Top Industrie, France). Cells were collected by centrifugation and boiled for 5 min

for lysis. The whole cell extracts were separated on 10% SDS-PAGE. The FtsZ-GFP proteins were detected with polyclonal anti-GFP (Thermo Fisher, 1: 10000 dilution), anti-FtsZ$_{Ec}$ (Agisera, 1:3000 dilution) or anti-FtsZ$_{Sb}$ (raised by ChinaPeptides, 1:3000 dilution) as first antibodies, and horseradish peroxidase conjugated goat anti-rabbit IgG as secondary antibody (Thermo Fisher). The CN/DAB substrate kit (Thermo Fisher) was used for the development.

2.4 *In-situ* fixation of *E. coli* cells and fluorescent microscope observation

The $E. coli$ cells expressing FtsZ-GFP were grown at 37°C for 5 h with shaking. Approximately 500 μL cultures were then transferred into 1 mL syringes containing a small stainless-steel bead. The syringes were assembled into the HHP $in-situ$ fixation apparatus and connected with the syringe containing 400 μL 10% paraformaldehyde as fixative. The HHP $in-situ$ fixation apparatus were incubated under atmospheric (0.1 MPa) or high (50 MPa) pressures for 5 h before the injection of the fixatives and fixation for 30 min. Ten microliter of fixed cells were taken for microscope observation. The phase-contrast and fluorescence images were taken using BX51 microscope (Olympus). The measurement of cellular length and counting number of cells

bearing different types of fluorescence were carried out with Fiji (Schindelin et al., 2012).

2.5 Protein purification

The pET plasmids were transformed into Rosetta™ (DE3) cells for protein expression and purification. Cells were grown at 37°C until OD_{600nm} reached 0.4. Isopropyl β-D-thiogalactoside was added to a final concentration of 0.5 mM. After 3 h' induction, cells were collected by centrifuge and washed twice with 20 mM Tris–HCl pH 8.0. The cell pellet from 1 L culture was resuspended in 100 mL lysis buffer (10 mM imidazole, 20 mM Tris–HCl, 500 mM NaCl) supplemented with Pierce™ protease inhibitor (Thermo Fisher) and lysed through sonication. The cellular lysis was centrifuged at 5000 rpm for 30 min at 4°C, and the supernatant was then loaded to 5 mL Ni^{2+}-agarose column (Sangon Biotech) pre-equilibrated with 10 mL lysis buffer. The column was washed with two bed-volumes of washing buffers containing 20 mM and 30 mM imidazole, respectively. The FtsZ was then eluted with 10 mL elution buffer containing 100 mM imidazole. The eluted fractions were analyzed by SDS-PAGE, pooled together, and dialyzed against Tris–HCl pH 8.0 and concentrated using Amicon® Ultra Centrifugal Filters (Millipore). The purified proteins were quantified with Pierce™ BCA Protein Assay Kits (Thermo Fisher).

2.6 FtsZ polymerization and TEM observation

In vitro polymerization assays were performed as described previously with slight modifications (Ishii et al., 2004). The reactions contained 50 mM KCl, 10 mM $MgCl_2$, 50 mM Tris–HCl pH 8.0, 2 mM GTP and 5 μM purified FtsZ proteins. For each assay, 500 μL reaction solution was transferred into 1 mL syringe containing a stainless-steel bead which was assembled into the *in-situ* fixation apparatus with another syringe containing 400 μL 10% glutaraldehyde as fixative. The apparatus was first incubated for 10 min under atmospheric pressure, then pressurized to 50 MPa or remained at 0.1 MPa for 5 h' incubation. The fixative was injected into the reaction syringe to allow fixation under corresponding pressure conditions for 30 min before decompression. All reactions were performed at ambient temperature. An aliquot of 10 μL fixed polymerization solutions were placed on carbon-coated copper grid and stained with 1% uranyl acetate. At least 8 grids were prepared for each assay and observed by electron microscopy (Hitachi HT7700). The number of FtsZ filaments on each grid were counted.

3 Results

3.1 Set up of a HHP *in-situ* fixation apparatus

The inhibitory effects of HHP on several bioprocesses, including cell division, are reversible, and the defects restores soon upon decompression (Ishii et al., 2004; Okuno et al., 2013; Hayashi et al., 2016). Therefore, it is important to either carry out the observations under HHP or have the cellular features well-preserved before

decompression (Nishiyama et al., 2010; Nishiyama, 2017; Yin et al., 2017; Bourges et al., 2020). *In-situ* HHP fixation systems have been applied by several groups (Chastain and Yayanos, 1991; Ishii et al., 2004; Moussa et al., 2007). In general, the fixative agent and the sample are separated in two chambers by a coverslip or a Parafilm membrane. To achieve effective fixation, the coverslip or membrane need to be broken with a weighted ball or needle and accompanied with rigorous shaking.

Here, we set up an *in-situ* fixation apparatus optimized for samples with small volumes (Figure 1A). The apparatus consists of a core unit, a pressure vessel, and a pressure controlling system. The core unit constitutes two syringes. Syringe A on the left contains fixative. Syringe B on the right, whose plug is removed, contains the sample to be fixed and a small stainless-steel bead for thorough mixing. The two syringes are separated by a stainless-steel ball, to prevent free exchange of solutions between the two syringes, and the three items are connected by a vinyl tube (Figure 1B and Supplementary Figure S1A). The core unit is installed onto a syringe rack and then placed into the high-pressure vessel (HP vessel) with the plug of syringe A against the piston of the HP vessel. To carry out HHP incubation and fixation, the system is pressurized by injecting water from the inlet on the right using a water pump (Figure 1C1). Upon completion of HHP incubation, water is injected from the inlet on the left, which pushes the piston rightwards, and consequently, injects the fixative from syringe A into syringe B (Figure 1C2). During this process, the pressure inside the HP vessel is maintained by the back pressure regulator. Finally, by inverting the pressure vessel, the fixative and sample in syringe B are thoroughly mixed by the small stainless-steel ball inside. The maximum working pressure of this apparatus is 60 MPa, and three replicates could be manipulated at a time.

To determine the volume of water required to move the piston and the volume of fixative injected into syringe B, we filled syringe A with a colored dye Coomassie blue and syringe B with water, and measured the absorbance of solution in syringe B after HHP incubation and "fixative" injection at 50 MPa (Supplementary Figure S1). By injecting 30 mL or 40 mL water into the HP vessel, the Coomassie blue in syringe A was hardly injected into syringe B (Supplementary Figures S1B,C). When 50 mL or 60 mL water were used, Coomassie blue from syringe A was injected into syringe B, and the final concentration of Coomassie blue in syringe B were 10.2 ± 5.8% and 21.8 ± 3.3%, in relative to the original Coomassie blue solution, respectively (Supplementary Figures S1D,E). Further increase the volume of water injected may risk of bending the syringe rack. Therefore, an injection of 60 mL water was utilized in this study, which guaranteed reproducible fixations with approximately 5 times diluted fixative.

3.2 Z-ring formed by FtsZ from piezophilic bacterium has better tolerance to HHP

We first compared the influence of HHP on Z-ring formation of three FtsZ proteins from strains with different pressure tolerance: one from an obligate piezophile that grown exclusively at HHP condition ($FtsZ_{Sb}$ from *S. benthica* DB21MT-2) and two from pressure sensitive strains ($FtsZ_{Ec}$ from *E. coli*, and $FtsZ_{So}$ from *S. oneidensis* MR-1). The FtsZ proteins were expressed in *E. coli* with a GFP-tag at C-terminal. The *E. coli* cells were grown aerobically
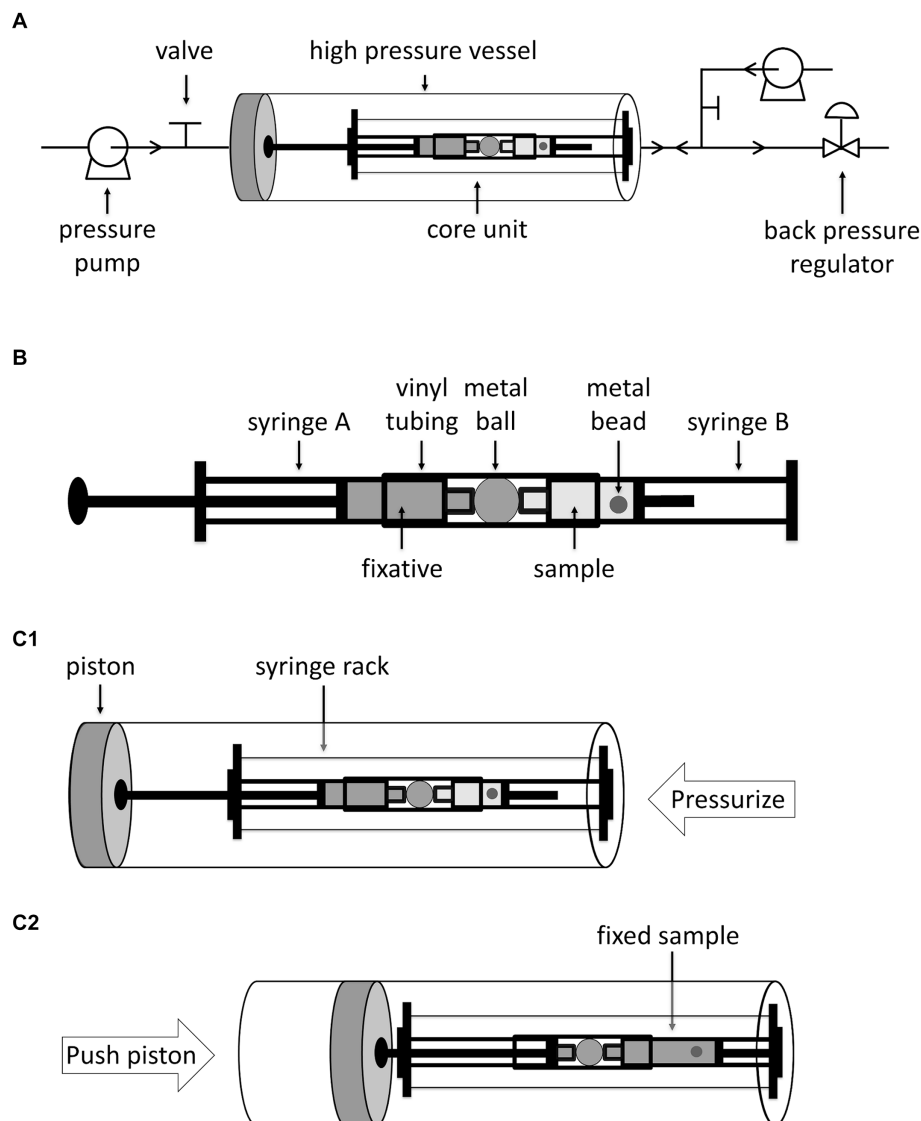
FIGURE 1
Diagrammatic sketch of *in-situ* fixation apparatus and its operation. Panel **A** shows the *in-situ* fixation apparatus, including the pipelines, the high pressure vessel, the core unit and other accessories. The arrows on the pipelines indicate the flow direction. Panel **B** shows a closer look at the core unit. Panel **C1**,**C2** shows the position of core unit in the high pressure vessel and operation of *in-situ* fixation apparatus. Water is injected from right inlet to pressurize the high pressure vessel. To inject fixative into sample, water is injected from left inlet which pushes the piston as well as the plunger of the syringe A rightwards.

under atmospheric pressure to allow maturation of fluorescent GFP before incubated under 0.1 MPa or 50 MPa, respectively. The expressions of FtsZ-GFP fusion proteins were confirmed by western-blot analysis. All three fusion proteins (FtsZ$_{Ec}$-GFP, FtsZ$_{So}$-GFP and FtsZ$_{Sb}$-GFP) were expressed at comparable level and no free GFP was detected suggesting that the fusion proteins remained stable under both pressure conditions, and the green fluorescence is exclusively related to the heterogeneously expressed FtsZs (Supplementary Figure S2A).

After 5 h' incubation under atmospheric pressure, the *E. coli* cells expressing all three FtsZ-GFP fusion proteins were mostly 2–4 μm short-rod shaped. Consistent with previous observation, incubation at 50 MPa impeded division of cells expressing FtsZ$_{Ec}$-GFP, and the majority of cells were filamentous with an average cellular length over 20 μm. In contrast, cells expressing FtsZ$_{So}$-GFP and FtsZ$_{Sb}$-GFP

remained short-rod shaped at incubation at 50 MPa, and the majority of cells were 2–6 μm in length (Figure 2 and Supplementary Figure S3).

The subcellular localization of different FtsZ proteins were examined with fluorescent microscope. In all three cultures tested, over 60% cells were fluorescent, and three types of fluorescence were observed. The sharp bands perpendicular to the long axis of cell was referred to as Z-ring-like fluorescence, which were most likely properly polymerized and located FtsZ-GFP filaments (Figures 2A1–A11, white arrows). The sporadic spots, spiral and filamentous patterns were collectively recognized as ectopic fluorescence, which indicated abnormal polymerization or localization of FtsZ-GFP (Figures 2A1–A11, yellow arrows). The homogenous fluorescence indicated free FtsZ-GFP subunits failed to polymerize (Figures 2A1–A11, blue arrows). When FtsZ$_{Ec}$-GFP was expressed, cells with Z-ring-like or homogenous fluorescence each accounted for 20% in cultures
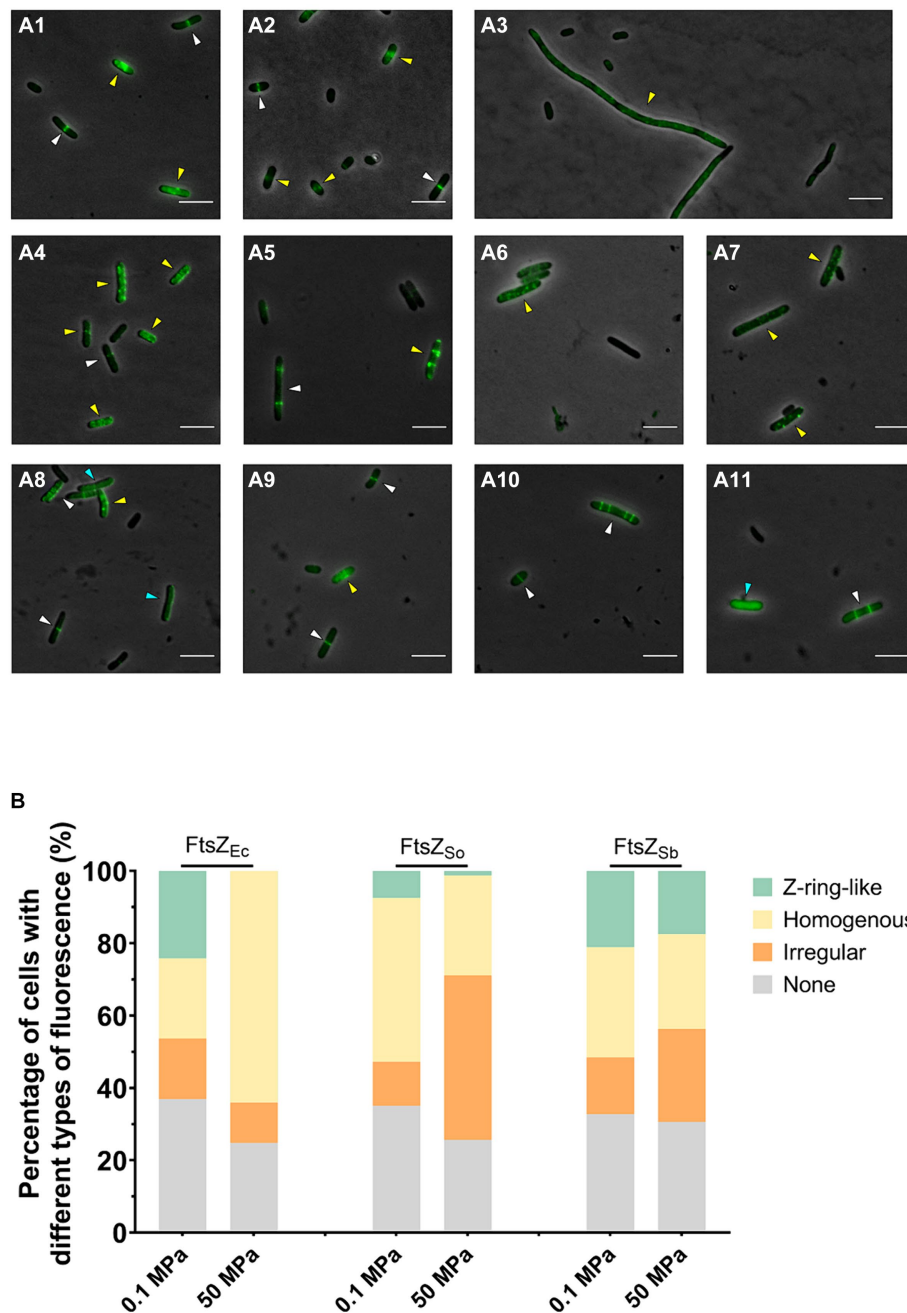
FIGURE 2
Effect of HHP on subcellular localization of FtsZ$_{Ec}$, FtsZ$_{So}$ and FtsZ$_{Sb}$. Panel **A** shows fluorescence in *E. coli* cells expressing different FtsZ proteins under ambient and high pressures. Panel **A1−A3** show cells expressing FtsZ$_{Ec}$-GFP incubated under 0.1 MPa **(A1,A2)** and 50 MPa **(A3)**; Panel **A4−A7** show cells expressing FtsZ$_{So}$-GFP incubated under 0.1 MPa **(A4,A5)** and 50 MPa **(A6,A7)**; Panel **A8−A11** show cells expressing FtsZ$_{Sb}$-GFP incubated under 0.1 MPa **(A8,A9)** and 50 MPa **(A10,A11)**. All scale bars indicate 5 μm. The white arrows indicate cells with Z-ring-like fluorescence, blue arrows indicate cells with homogenous fluorescence and yellow arrows indicate cells with ectopic fluorescence. Panel **B** shows the average percentage of cells with different types of fluorescence. The data were collected from three independent assays. In each assay, over 300 cells were analyzed for each culture.

incubated under atmospheric pressure, while cells with Z-ring-like fluorescence can hardly be observed after incubation under 50 MPa and the percentage of cells with homogenous fluorescence increased remarkably to approximately 60% (Figures 2A1–A1,B). In cells expressing FtsZ$_{So}$-GFP, the proportion of cells with Z-ring-like fluorescence decreased from 7% under atmospheric pressure to around 1% under 50 MPa, along with an increase of cells with ectopic

fluorescence from 12 to 46% (Figures 2A4–A7,B). On the contrary, the fluorescence patterns of cells expressing FtsZ$_{Sb}$-GFP were stable under both pressures. Cells exhibiting Z-ring-like fluorescence accounted for 21.1% at 0.1 MPa and 17.5% at 50 MPa, respectively (Figures 2A8–A11,B). These observations suggested that both FtsZ$_{So}$ and FtsZ$_{Sb}$ were able to form or incorporate into Z-ring under atmospheric pressure. Moreover, unlike the Z-rings composed of FtsZ from

pressure-sensitive strains, which were prone to depolymerize or aggregate under high pressure conditions, the Z-rings composed of FtsZ from the obligate piezophile ($FtsZ_{Sb}$) were more resistant to high pressure *in vivo*.

3.3 $FtsZ_{Sb}$ filaments are more stable under high pressures *in vitro*

Both the intrinsic property of FtsZ itself and its interaction with division factors such as ZapAB affect stability of FtsZ polymer *in vivo* (Ebersbach et al., 2008; Durand-Heredia et al., 2011; Galli and Gerdes, 2012). Here we focused on the influence of HHP on FtsZ polymerization and with purified FtsZ proteins we examined the stability of different FtsZ filaments *in vitro*. Upon incubation under atmospheric pressure condition, bundles of filaments could be observed for both $FtsZ_{So}$ and $FtsZ_{Sb}$. To be more specific, the average numbers of filaments per grid were 7.6 and 7.2, for $FtsZ_{So}$ and $FtsZ_{Sb}$, respectively (Figures 3A1,B1,C). After incubation at 50 MPa, filament of $FtsZ_{So}$ was hardly observed, we found only 3 bundles of $FtsZ_{So}$ filaments from 9 grids, while 20 bundles of $FtsZ_{Sb}$ filaments were found on 10 grids (Figures 3A2,B2,C). Although the number of filament bundles cannot be used to quantify polymerization of FtsZ subunits, the apparent different performance between $FtsZ_{So}$ and $FtsZ_{Sb}$ filaments suggested a higher stability of $FtsZ_{Sb}$ filaments or stronger polymerization of $FtsZ_{Sb}$ under HHP conditions. Moreover, the difference between $FtsZ_{So}$ and $FtsZ_{Sb}$ was determined by their intrinsic properties.

3.4 N-terminal GTPase domain plays an important role in HHP adaptation of $FtsZ_{Sb}$

Both *in vivo* and *in vitro* assays suggested that FtsZ from obligate piezophile ($FtsZ_{Sb}$) was better adapted to HHP than its counterpart

from pressure sensitive strain ($FtsZ_{So}$). A sequence alignment was performed using FtsZ proteins from 5 representative *Shewanella* strains with different pressure tolerance: the obligate piezophilic strains DB21MT-2 and KT99, piezophilic strain DSS12, pressure tolerant strain WP3 and pressure sensitive strain MR-1 (Figure 4A). They all comprised three domains: a highly conserved N-terminal GTPase domain (amino acids 1 to 316, the numbers are based on the sequence of $FtsZ_{Sb}$), a divergent linker region (amino acids 317 to 372), and a conserved C-terminal domain (amino acids 373 to 388). To understand the contribution of each domain to HHP adaptation, we constructed three chimeric FtsZ proteins by replacing each of the three domains in pressure-tolerant $FtsZ_{Sb}$ with corresponding segment from pressure sensitive $FtsZ_{So}$, and resulted in $FtsZ_{So-N}$, $FtsZ_{So-L}$ and $FtsZ_{So-C}$, respectively (Table 1 and Figure 4B).

The three chimeric FtsZ proteins were expressed with GFP tag in *E. coli* cells (Supplementary Figure S2B). Similar to cells expressing the wild-type $FtsZ_{Sb}$, cells containing chimeric FtsZ proteins were short-rod shaped, and the majority (around 80%) were fluorescent (Supplementary Figure S4). Under atmospheric pressure, cells expressing $FtsZ_{So-N}$-GFP and $FtsZ_{So-L}$-GFP had similar fluorescent patterns: cells exhibiting Z-ring-like, ectopic and homogenous fluorescence accounted for 10, 30 and 40%, respectively. In cells expressing $FtsZ_{So-C}$-GFP, the proportion of Z-ring-like and ectopic fluorescent cells were relatively lower (accounted for 5 and 16%, respectively) while homogenous fluorescent cells increased to approximately 60% (Table 2). After incubation under 50 MPa, Z-ring-like fluorescent cells could be observed in all three strains, but their proportions were affected differently by HHP (Table 2). In cells expressing $FtsZ_{So-N}$-GFP, incubation at 50 MPa clearly decreased the ratio of Z-ring-like fluorescent cells ($10.2 \pm 4.5\%$ at 0.1 MPa versus $5.8 \pm 1.4\%$ at 50 MPa), along with an increase of the cells with ectopic fluorescence ($33.1 \pm 13.3\%$ at 0.1 MPa versus $43.9 \pm 4.6\%$ at 50 MPa). When $FtsZ_{So-L}$-GFP was expressed, the fluorescent profile was hardly affected by changing of pressure, which was similar to the wild-type $FtsZ_{Sb}$-GFP. Meanwhile, a higher ratio of cells with Z-ring-like
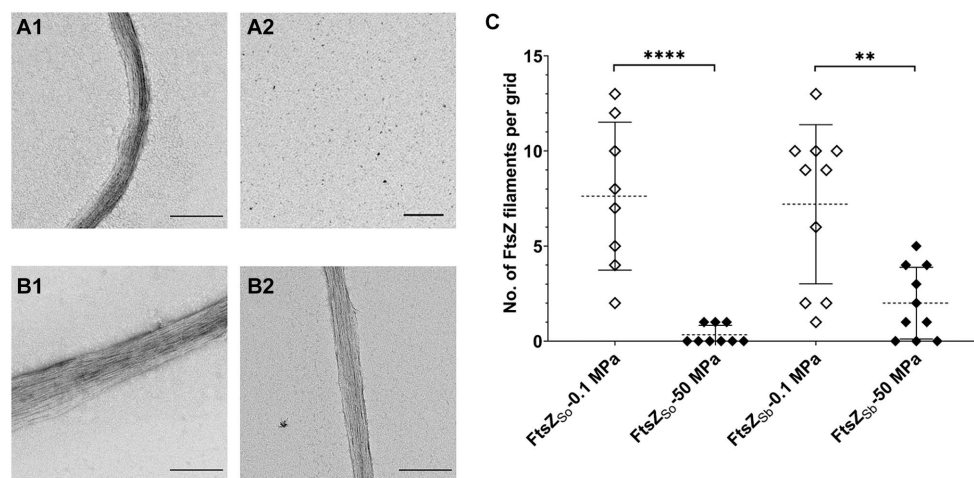
FIGURE 3
Effect of HHP on FtsZ polymerization *in vitro*. Panel **A** shows filaments of purified $FtsZ_{So}$ incubated at 0.1 MPa (**A1**) and 50 MPa (**A2**), panel **B** shows filaments of purified $FtsZ_{Sb}$ incubated at 0.1 MPa (**B1**) and 50 MPa (**B2**), respectively. The scale bar indicates 2 μm. Panel **C** shows number of FtsZ filaments observed on each grid. Mean value and standard deviation are indicated by dashed lines and solid lines. Statistical analysis was carried out using two-tailed unpaired t-test: **** $p < 0.0001$, ** $p < 0.01$.

FIGURE 4
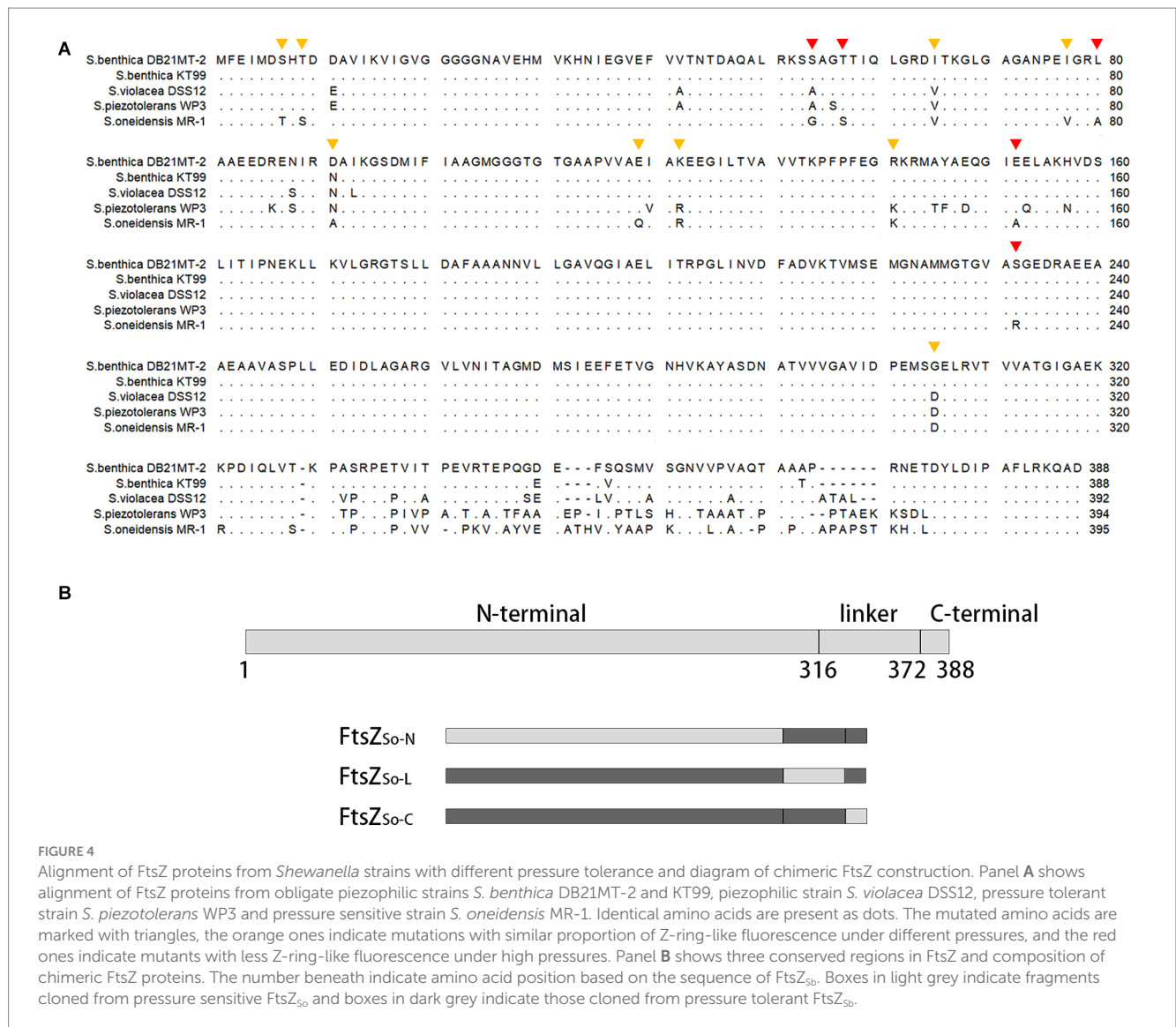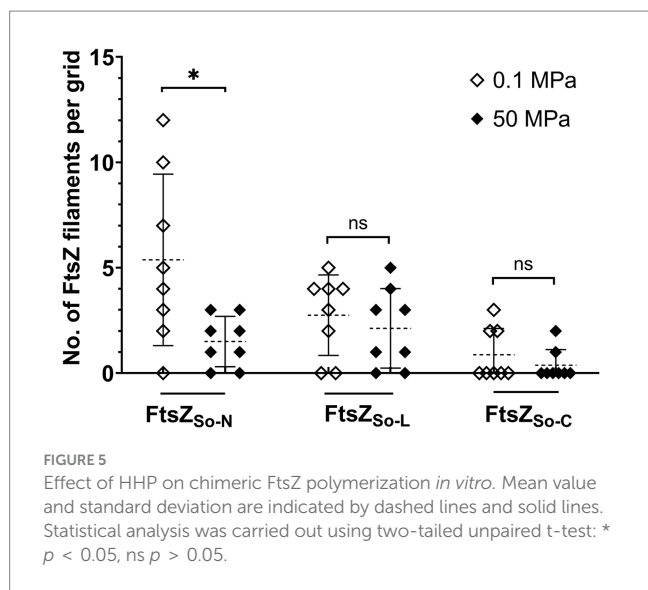Alignment of FtsZ proteins from *Shewanella* strains with different pressure tolerance and diagram of chimeric FtsZ construction. Panel **A** shows alignment of FtsZ proteins from obligate piezophilic strains *S. benthica* DB21MT-2 and KT99, piezophilic strain *S. violacea* DSS12, pressure tolerant strain *S. piezotolerans* WP3 and pressure sensitive strain *S. oneidensis* MR-1. Identical amino acids are present as dots. The mutated amino acids are marked with triangles, the orange ones indicate mutations with similar proportion of Z-ring-like fluorescence under different pressures, and the red ones indicate mutants with less Z-ring-like fluorescence under high pressures. Panel **B** shows three conserved regions in FtsZ and composition of chimeric FtsZ proteins. The number beneath indicate amino acid position based on the sequence of FtsZ$_{Sb}$. Boxes in light grey indicate fragments cloned from pressure sensitive FtsZ$_{So}$ and boxes in dark grey indicate those cloned from pressure tolerant FtsZ$_{Sb}$.

TABLE 2 Sub-cellular localization of chimeric FtsZ under different pressure conditions.

FtsZ	Pressures (MPa)	Ratio of different types of fluorescence (%)				No. of cells analyzed
		Z-ring-like	Homogenous	Ectopic	None	
FtsZ$_{So-N}$	0.1	10.2 ± 4.5	37.0 ± 16.9	33.1 ± 13.3	19.7 ± 8.4	985
	50	5.8 ± 1.4	34.5 ± 6.4	43.9 ± 4.6	15.8 ± 9.7	1,043
FtsZ$_{So-L}$	0.1	11.9 ± 6.3	36.5 ± 4.5	27.8 ± 5.9	23.7 ± 14.8	1,038
	50	11.3 ± 4.1	37.7 ± 3.6	26.0 ± 6.0	25.0 ± 11.2	1,021
FtsZ$_{So-C}$	0.1	4.7 ± 1.1	59.8 ± 3.6	15.6 ± 9.7	19.8 ± 12.1	698
	50	9.6 ± 3.5	54.2 ± 0.6	14.6 ± 7.5	21.6 ± 11.6	790

fluorescence was observed under HHP condition when FtsZ$_{So-C}$-GFP was expressed (4.7 ± 1.1% at 0.1 MPa versus 9.6 ± 3.5% at 50 MPa). These observations suggested that, compared to FtsZ$_{So}$, the higher HHP tolerance of Z-ring formed by FtsZ$_{Sb}$ was largely due to its N-terminal GTPase domain. The linker domain hardly affected the HHP tolerance, while the C-terminal domain from FtsZ$_{So}$ may increase the HHP stability of Z-ring *in vivo*.

The HHP stability of chimeric FtsZ filaments was further examined *in vitro*. For samples incubated under atmospheric pressure, filament bundles of FtsZ$_{So-N}$ and FtsZ$_{So-L}$ could be observed on most grids, while filaments of FtsZ$_{So-C}$ can only be found occasionally. As expected, the influence of elevated pressure varied from different chimeric FtsZ proteins (Figure 5). At atmospheric pressure, an average of 5.4 bundles of filaments

FIGURE 5
Effect of HHP on chimeric FtsZ polymerization *in vitro*. Mean value and standard deviation are indicated by dashed lines and solid lines. Statistical analysis was carried out using two-tailed unpaired t-test: * $p < 0.05$, ns $p > 0.05$.

FIGURE 6
Mapping of mutants on the predicted structure of $FtsZ_{Sb}$ and the effect of HHP on subcellular localization of mutated $FtsZ_{Sb}$. Panel A1,A2 show the mutated amino acids on $FtsZ_{Sb}$. The amino acid numbers refer to the $FtsZ_{Sb}$ sequence. Panel B shows the ratio of cells exhibiting Z-ring-like fluorescence under 0.1 MPa (grey bars) and under 50 MPa (red bars). The mutated $FtsZ_{Sb}$ whose localization was severely affected by high pressure were marked with #.

composed of $FtsZ_{So-N}$ could be found on a grid, and in one case, a maximum of 12 bundles of filaments were observed. Meanwhile, no more than three bundles of filaments could be visualized with $FtsZ_{So-N}$ incubated under 50 MPa. For filaments formed by $FtsZ_{So-L}$ and $FtsZ_{So-C}$, no significant difference was found between incubation at atmospheric and high pressure conditions. Collectively, these results indicated that the N-terminal GTPase domain played an important role in Z-ring formation and polymerization of FtsZ filaments under high pressures.

3.5 Mutation of five amino acids from N-terminal GTPase domain reduces pressure tolerance of $FtsZ_{Sb}$

A closer examination of the N-terminal GTPase domains from $FtsZ_{So}$ and $FtsZ_{Sb}$ showed 14 different amino acids, all of them were exposed on the surface (indicated by orange and red arrows in Figure 4A and Figures 6A1,A2). By site-directed mutagenesis, we replaced each of the 14 amino acids in $FtsZ_{Sb}$ with the corresponding amino acid from $FtsZ_{So}$ (Table 1). Western-blot showed that the expression and stability of mutant $FtsZ_{Sb}$-GFP fusion proteins in *E. coli* cells were not affected by elevated pressure (Supplementary Figure S2C). The localization of the mutated $FtsZ_{Sb}$ at 0.1 MPa and 50 MPa were then examined (Figure 6B and Table 3). In general, cells with Z-ring-like fluorescence accounted for 5 to 15% under atmospheric pressure condition, which was lower compared to cells expressing the wild-type $FtsZ_{Sb}$ protein (approximately 20%). Among all the mutant $FtsZ_{Sb}$, D91A had the lowest ratio of Z-ring-like fluorescent cells of 1.3% under atmospheric pressure, and higher amount of non-fluorescent cell and cells with ectopic fluorescence. Mutant T9S and T57S were also deficient in Z-ring formation under atmospheric pressure, the ratio of Z-ring-like fluorescent cell was 2.7%, and over half of the populations exhibited homogenous fluorescence.
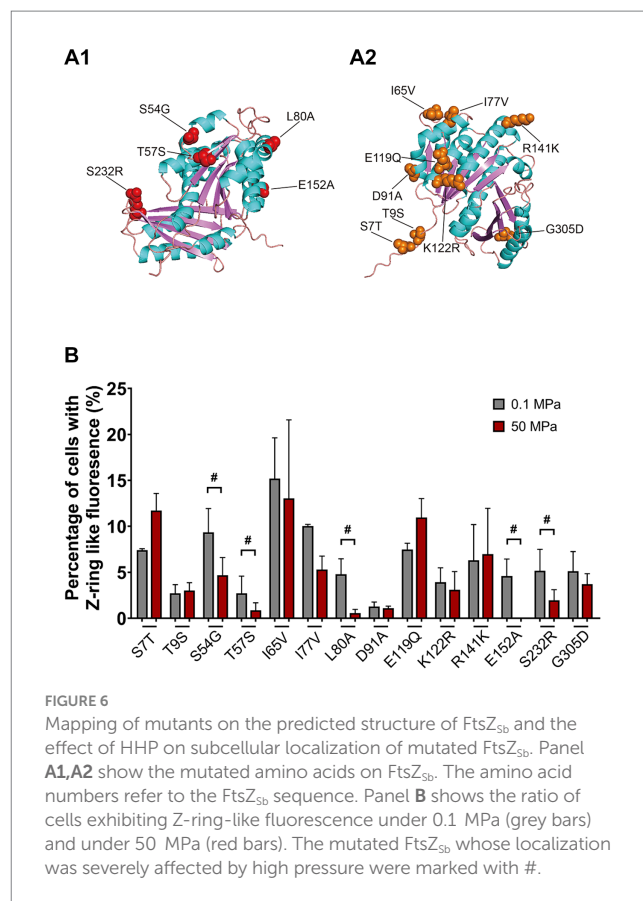
Upon incubation under HHP, the ratio of cells with Z-ring-like fluorescent slightly increased in mutant S7T and E119Q, from around 7 to 11%. For the rest of the mutants, the ratio of cells exhibiting Z-ring-like fluorescence decreased at different degrees. In 7 mutants (T9S, I65V, I77V, D91A, K122R, R141K, and G305D), cultures at 50 MPa and 0.1 MPa had comparable ratio (less than 2-fold changes) of Z-ring-like fluorescent cell. It suggested that elevated pressure had little influence on their Z-ring formation, resembling the wild-type $FtsZ_{Sb}$ protein. On the other hand, HHP decreased the ratio of cells exhibiting Z-ring-like fluorescence by over 2-fold in the other five mutants (S54G, T57S, L80A, E152A, and S232R), indicating a more critical role of these amino acids in maintaining the Z-ring structure under HHP condition. Remarkably, in cultures of L80A and E152A, around 5% cells bore Z-ring-like fluorescence under atmospheric pressure, while the ratio decreased to less than 1% under high pressure condition.

Collectively, by applying a novel HHP *in-situ* fixation apparatus, we examined the pressure tolerance of cytoskeleton protein FtsZ from bacterial strains inhabiting different water depth. Our results suggested that $FtsZ_{Sb}$ from obligately piezophilic strain *S. benthica* DB21MT-2 inhabiting the bottom of the Mariana Trench has better pressure tolerance than its homologues from shallow water species with respect to Z-ring formation *in vivo* and FtsZ polymerization *in vitro*. Differences in pressure tolerance of FtsZ was largely attributed to the N-terminal GTPase domain and five amino acids were probably involved in the adaptation of FtsZ to the HHP environment.

TABLE 3 Effect of HHP on sub-cellular localization of mutated FtsZ$_{Sb}$.

FtsZ$_{Sb}$ mutant	Pressures (MPa)	Ratio of different types of fluorescence (%)				No. of cells analyzed
		Septum	Homogenous	Ectopic	None	
S7T	0.1	7.4 ± 0.1	40.1 ± 3.3	41.1 ± 9.6	11.4 ± 6.1	687
	50	11.7 ± 1.8	43.3 ± 14.7	31.0 ± 18.4	14.0 ± 5.6	713
T9S	0.1	2.7 ± 0.9	59.3 ± 0.8	25.1 ± 9.3	12.9 ± 9.5	695
	50	3.0 ± 0.8	57.4 ± 2.4	20.6 ± 6.4	19.0 ± 4.8	689
S54G#	0.1	9.4 ± 2.6	60.0 ± 5.1	15.3 ± 3.6	15.3 ± 5.5	996
	50	4.7 ± 1.9	65.4 ± 9.7	20.9 ± 5.2	9.0 ± 6.5	920
T57S#	0.1	2.7 ± 1.9	51.8 ± 11.3	22.1 ± 11.4	23.4 ± 17.5	1,026
	50	0.9 ± 0.8	71.2 ± 7.6	14.0 ± 6.0	13.9 ± 3.9	1,056
I65V	0.1	15.2 ± 4.4	40.8 ± 2.8	25.0 ± 21.3	19.0 ± 14.0	618
	50	13.0 ± 8.5	56.4 ± 9.5	26.0 ± 18.2	4.5 ± 0.1	618
I77V	0.1	10.0 ± 0.2	49.4 ± 20.9	23.7 ± 12.7	16.9 ± 8.0	628
	50	5.3 ± 1.5	61.9 ± 25.4	19.3 ± 13.5	13.4 ± 10.4	660
L80A#	0.1	4.8 ± 1.7	40.4 ± 19.3	16.6 ± 3.9	38.2 ± 24.9	730
	50	0.6 ± 0.4	57.0 ± 10.0	18.2 ± 5.5	24.4 ± 4.0	674
D91A	0.1	1.3 ± 0.5	26.6 ± 8.7	33.5 ± 6.0	38.7 ± 2.2	626
	50	1.1 ± 0.2	37.9 ± 4.7	19.8 ± 4.6	41.2 ± 0.1	641
E119Q	0.1	7.5 ± 0.7	51.5 ± 1.9	24.8 ± 1.4	16.2 ± 4.0	629
	50	11.0 ± 2.0	45.0 ± 3.7	13.6 ± 0.5	30.4 ± 6.2	729
K122R	0.1	5.3 ± 2.6	36.6 ± 13.0	21.5 ± 8.6	36.7 ± 8.2	674
	50	3.5 ± 1.6	52.6 ± 15.5	20.9 ± 6.6	23.1 ± 13.1	663
R141K	0.1	6.3 ± 3.9	39.9 ± 11.1	22.7 ± 1.4	31.1 ± 8.6	617
	50	7.0 ± 5.0	46.3 ± 7.9	13.3 ± 0.6	33.4 ± 2.3	632
E152A#	0.1	4.6 ± 1.9	46.1 ± 22.1	23.4 ± 7.7	25.8 ± 12.6	671
	50	0.0 ± 0.0	58.5 ± 21.0	13.2 ± 1.6	28.3 ± 22.6	666
S232R#	0.1	6.5 ± 0.6	69.5 ± 6.0	9.4 ± 4.0	14.6 ± 2.6	949
	50	2.4 ± 1.1	75.4 ± 2.4	12.5 ± 3.3	9.6 ± 6.8	924
G305D	0.1	5.1 ± 2.1	50.2 ± 17.6	19.7 ± 1.0	25.0 ± 18.7	636
	50	3.7 ± 1.1	46.8 ± 2.6	13.6 ± 3.2	35.9 ± 6.9	619

#Indicated mutated FtsZ$_{Sb}$ that form less Z-ring-like fluorescence under HHP condition.

4 Discussion

It is now established that the cytoskeleton of both prokaryotes and eukaryotes are vulnerable to HHP, with microtubules dissociating under HHP in both *in vivo* and *in vitro* conditions (Salmon, 1975a,b; Messier and Seguin, 1978; Bourns et al., 1988; Ishii et al., 2004; Arai et al., 2008; Nishiyama et al., 2010; Hayashi et al., 2016). A simulation study conducted by Dicken et al. demonstrated that the difference in Gibbs free energy between monomer and dimer of *Methanococcus jannaschii* FtsZ decreases with pressure, which could potentially explain the HHP-induced depolymerization of FtsZ (Dicken et al., 2015). Recent study suggests that depolymerization of microtubules induced by HHP is largely due to internal cavities and voids. Furthermore, compared to longitudinal interactions, the lateral interactions are more susceptible to HHP (Gao et al., 2018).

The functional Z-ring is a discontinuous structure composed of a bundle of FtsZ filaments formed through lateral filament interactions (Fu et al., 2010; Szwedziak et al., 2014). Earlier studies have demonstrated that lateral interactions enable the FtsZ protofilaments to associate and form the Z-ring structure at the division site. Disruption of the lateral interaction may lead to a failure of cell division (Monahan et al., 2009; Shin et al., 2013; Guan et al., 2018). The lateral interface of FtsZ is composed of residues in helices H3, H4 and H5 in the N-terminal GTPase domain, and the C-terminal variable region (Buske and Levin, 2012; Guan et al., 2018). In this study, we found that mutation of two residues in the helices H3 and H5 (L80A and E152A) of FtsZ$_{Sb}$, which were close to the lateral interface, led to significant defect in HHP tolerance. In these two mutants, Z-ring-like fluorescence was observed in 5% of cells under atmospheric pressure, which was slightly less than the wild-type FtsZ$_{Sb}$, but almost undetectable in cells incubated under 50 MPa. It is thus speculated that longer side chains of these two residues enhance the lateral interaction between FtsZ filaments under HHP condition, thereby reinforcing the stability of FtsZ filaments and the Z-ring.

In addition to the intrinsically driven lateral interactions, modulatory proteins such as ZapABCDE have been documented to promote the lateral interactions between FtsZ filaments and stabilize the Z-ring (Durand-Heredia et al., 2011, 2012; Galli and Gerdes, 2012; Marteyn et al., 2014; Schumacher et al., 2016, 2017). It is now understood that FtsZ interacts with ZapA through its C-terminal region and the two lysines in its GTPase domain are close to the binding site and are cross-linked with ZapA (K51 and K66 in FtsZ$_{Ec}$, corresponding to K52 and K67 in FtsZ$_{Sb}$). These two lysines are highly conserved across *Shewanella* species analyzed, regardless of whether they inhabit the shallow or deep water. However, our findings showed that residues between these two lysines may play a significant role in the adaptation to HHP. The septum localizations of mutant FtsZ S54G and T57S were notably impaired by HHP, as only half or one-third cells displaying Z-ring-like fluorescence under 50 MPa compared to cultures incubated at atmospheric pressure. One possible explanation for this is that these mutations disrupted the interaction between FtsZ and ZapA, thereby weakening the stability of FtsZ$_{Sb}$. It should be noted that these residues are also in the vicinity of the GTP binding site, and further experimental evidence is required to elucidate their contribution in the HHP adaptation of FtsZ$_{Sb}$.

Another possible factor influencing HHP tolerance could be the GTPase activity. Changes in GTPase activity can impact both the morphology and organization of FtsZ filaments, as well as the rate of treadmilling, which is essential for Z-ring assembly and cell division (Lu et al., 2001; Jaiswal et al., 2010; Arjes et al., 2015; Lyu et al., 2016; Yang et al., 2017). While there have been no previous reports on the effect of HHP on the GTPase activity of tubulin, numerous studies have demonstrated that the GTP binding and GTP hydrolysis of the guanine nucleotide binding proteins, such as those involved in cellular signaling pathways, are sensitive to elevated pressure (Siebenaller and Murray, 1994; Siebenaller, 2003). Given that several mutations in the GTPase domain of FtsZ$_{Sb}$ led to decreased tolerance to HHP, we have attempted to directly measure the GTPase activity of different FtsZ proteins under elevated pressures. Unfortunately, accurately adding solutions of several microliters to the reaction system while maintaining pressure proved to be a significant challenge, leaving this hypothesis untested.

In this study, we noticed that after 24 h' incubation under 50 MPa, cells expressing FtsZ$_{Sb}$ were also elongated as the wild-type *E. coli* cells, even though the sharp Z-ring-like fluorescence could be observed (Supplementary Figures S5A2,A3,B2,B3). This observation suggested that a pressure tolerant FtsZ alone is not sufficient to restore cells division under high pressure condition. The complex process of cell division encompasses the positioning of FtsZ, protein recruitment and divisome assembly, constriction, hydrolysis and synthesis of peptidoglycan, with any disruption potentially leading to impaired cell division (Du et al., 2019). In addition, given that the majority of divisome components are anchored on inner membrane, it is not surprising that the physicochemical property of cellular membrane is also important for cell division (Kawamoto et al., 2009). It is well known that HHP decreases membrane fluidity which may impair the activity of membrane proteins and membrane associated bioprocesses (Welch and Bartlett, 1998; Abe, 2013; Tamby et al., 2023). Previous study showed that deep-sea piezophilic bacteria deficient of eicosapentaenoic acid are able to form Z-ring but fail in nucleoids

partition and cell division under HHP condition. This suggested a disruption at the late stage of cell division (Kawamoto et al., 2011). The saturated fatty acids such as stearic acid and palmitic acid are the predominant fatty acids in *E.coli* cells (McGarrity and Armstrong, 1981). Meanwhile, monounsaturated acids account for 50–60% of total fatty acids in obligately piezophilic bacteria such as *Shewanella benthica* DB21MT-2 (Fang et al., 2004). The differences in fatty acids may also be a reason for the failure of division of *E.coli* cells under HHP. Therefore, even though FtsZ were correctly translocated to the septum and formed the Z-ring-like structure, the influence of HHP imposed on other protein components and membrane may impede division of *E. coli* cells under high pressures. Taken together, this study showed that FtsZ from the obligately piezophilic strain exhibits superior pressure tolerance and identified key residues for the adaptation of FtsZ to HHP. Yet, it is crucial to examine the impact of HHP on not only FtsZ but also other proteins involved in cell division, to fully comprehend this intricate process under extreme HHP environments.

Data availability statement

The raw data supporting the conclusions of this article will be made available by the authors, without undue reservation.

Author contributions

X-HC: Data curation, Formal analysis, Investigation, Methodology, Writing – review & editing. Y-CW: Data curation, Formal analysis, Investigation, Methodology, Writing – review & editing. X-GL: Methodology, Writing – review & editing, Supervision. X-QQ: Investigation, Project administration, Writing – review & editing. L-FW: Conceptualization, Funding acquisition, Supervision, Writing – review & editing. W-JZ: Conceptualization, Funding acquisition, Investigation, Supervision, Writing – original draft, Writing – review & editing.

Funding

Conflict of interest

The authors declare that the research was conducted in the absence of any commercial or financial relationships that could be construed as a potential conflict of interest.

The author(s) declared that they were an editorial board member of Frontiers, at the time of submission. This had no impact on the peer review process and the final decision.

Publisher's note

All claims expressed in this article are solely those of the authors and do not necessarily represent those of their affiliated organizations, or those of the publisher, the editors and the reviewers. Any

product that may be evaluated in this article, or claim that may be made by its manufacturer, is not guaranteed or endorsed by the publisher.

Supplementary material

The Supplementary material for this article can be found online at: https://www.frontiersin.org/articles/10.3389/fmicb.2024.1441398/full#supplementary-material

References

Abe, F. (2013). Dynamic structural changes in microbial membranes in response to high hydrostatic pressure analyzed using time-resolved fluorescence anisotropy measurement. *Biophys. Chem.* 183, 3–8. doi: 10.1016/j.bpc.2013.05.005

Adams, D. W., and Errington, J. (2009). Bacterial cell division: assembly, maintenance and disassembly of the Z ring. *Nat. Rev. Microbiol.* 7, 642–653. doi: 10.1038/nrmicro2198

Aertsen, A., and Michiels, C. W. (2005). Mrr instigates the SOS response after high pressure stress in *Escherichia Coli*: Mrr induced SOS response in *E. coli. Mol. Microbiol.* 58, 1381–1391. doi: 10.1111/j.1365-2958.2005.04903.x

Allen, E. E., and Bartlett, D. H. (2022). "Structure and regulation of the Omega-3 polyunsaturated fatty acid synthase genes from the Deep-Sea bacterium Photobacterium Profundum strain SS9". *Microbiology.* 148, 1903–1913. doi: 10.1099/00221287-148-6-1903

Allen, E. E., Facciotti, D., and Bartlett, D. H. (1999). Monounsaturated but not polyunsaturated fatty acids are required for growth of the Deep-Sea bacterium *Photobacterium Profundum* SS9 at high pressure and low temperature. *Appl. Environ. Microbiol.* 65, 1710–1720. doi: 10.1128/AEM.65.4.1710-1720.1999

Arai, S., Kawarai, T., Arai, R., Yoshida, M., Furukawa, S., Ogihara, H., et al. (2008). Cessation of cytokinesis in Schizosaccharomyces Pombe during growth after release from high hydrostatic pressure treatment. *Biosci. Biotechnol. Biochem.* 72, 88–93. doi: 10.1271/bbb.70451

Arjes, H. A., Lai, B., Emelue, E., Steinbach, A., and Levin, P. A. (2015). Mutations in the bacterial cell division protein FtsZ highlight the role of GTP binding and longitudinal subunit interactions in assembly and function. *BMC Microbiol.* 15:209. doi: 10.1186/s12866-015-0544-z

Bisson-Filho, A. W., Hsu, Y.-P., Squyres, G. R., Kuru, E., Fabai, W., Jukes, C., et al. (2017). Treadmilling by FtsZ filaments drives peptidoglycan synthesis and bacterial cell division. *Science* 355, 739–743. doi: 10.1126/science.aak9973

Bourges, A. C., Lazarev, A., Declerck, N., Rogers, K. L., and Royer, C. A. (2020). Quantitative high-resolution imaging of live microbial cells at high hydrostatic pressure. *Biophys. J.* 118, 2670–2679. doi: 10.1016/j.bpj.2020.04.017

Bourns, B., Franklin, S., Cassimeris, L., and Salmon, E. D. (1988). High hydrostatic pressure effects in vivo: changes in cell morphology, microtubule assembly, and actin organization. *Cell Motil.* 10, 380–390. doi: 10.1002/cm.970100305

Bravim, F., De, J. M., Freitas, A. A., Fernandes, R., and Fernandes, P. M. B. (2010). High hydrostatic pressure and the cell membrane: stress response of *Saccharomyces Cerevisiae*. *Ann. N. Y. Acad. Sci.* 1189, 127–132. doi: 10.1111/j.1749-6632.2009.05182.x

Buske, P. J., and Levin, P. A. (2012). Extreme C terminus of bacterial cytoskeletal protein FtsZ plays fundamental role in assembly independent of modulatory proteins. *J. Biol. Chem.* 287, 10945–10957. doi: 10.1074/jbc.M111.330324

Buske, P. J., and Levin, P. A. (2013). A flexible C-terminal linker is required for proper FtsZ assembly in vitro and Cytokinetic ring formation in vivo. *Mol. Microbiol.* 89, 249–263. doi: 10.1111/mmi.12272

Chastain, R. A., and Yayanos, A. A. (1991). Ultrastructural changes in an Obligately barophilic marine bacterium after decompression. *Appl. Environ. Microbiol.* 57, 1489–1497. doi: 10.1128/aem.57.5.1489-1497.1991

Dai, J., Li, X.-G., Zhang, T.-Y., Chen, H., Zhang, W.-J., Li, D., et al. (2024). Illuminating a bacterial adaptation mechanism: infrared-driven cell division in Deep-Sea hydrothermal vent environments. *Innovation Geosci.* 2, 100050–100010. doi: 10.59717/j.xinn-geo.2024.100050

Dicken, S. M., Nepal, S., and Kumar, P. (2015). Polymerization of FtsZ at high pressures: a molecular dynamics study. *Biophys. J.* 108:468a. doi: 10.1016/j.bpj.2014.11.2559

Du, S., Henke, W., Pichoff, S., and Lutkenhaus, J. (2019). How FtsEX localizes to the Z ring and interacts with FtsA to regulate cell division. *Mol. Microbiol.* 112, 881–895. doi: 10.1111/mmi.14324

Durand-Heredia, J., Rivkin, E., Fan, G., Morales, J., and Janakiraman, A. (2012). Identification of ZapD as a cell division factor that promotes the assembly of FtsZ in *Escherichia Coli. J. Bacteriol.* 194, 3189–3198. doi: 10.1128/JB.00176-12

Durand-Heredia, J. M., Yu, H. H., De Carlo, S., Lesser, C. F., and Janakiraman, A. (2011). Identification and characterization of ZapC, a stabilizer of the FtsZ ring in *Escherichia Coli. J. Bacteriol.* 193, 1405–1413. doi: 10.1128/JB.01258-10

Ebersbach, G., Galli, E., Møller-Jensen, J., Löwe, J., and Gerdes, K. (2008). Novel coiled-coil cell division factor ZapB stimulates Z ring assembly and cell division. *Mol. Microbiol.* 68, 720–735. doi: 10.1111/j.1365-2958.2008.06190.x

Fang, J., Kato, C., Sato, T., Chan, O., and McKay, D. (2004). Biosynthesis and dietary uptake of polyunsaturated fatty acids by Piezophilic Bacteria. *Comp. Biochem. Physiol. B: Biochem. Mol. Biol.* 137, 455–461. doi: 10.1016/j.cbpc.2004.01.009

Fu, G., Huang, T., Buss, J., Coltharp, C., Hensel, Z., and Xiao, J. (2010). In vivo structure of the *E. coli* FtsZ-ring revealed by Photoactivated localization microscopy (PALM). *PLoS ONE* 5:e12680. doi: 10.1371/journal.pone.0012680

Galli, E., and Gerdes, K. (2012). FtsZ-ZapA-ZapB Interactome of *Escherichia Coli. J. Bacteriol.* 194, 292–302. doi: 10.1128/JB.05821-11

Gao, M., Berghaus, M., Möbitz, S., Schuabb, V., Erwin, N., Herzog, M., et al. (2018). On the origin of microtubules' high-pressure sensitivity. *Biophys. J.* 114, 1080–1090. doi: 10.1016/j.bpj.2018.01.021

Gardner, K. A. J. A., Moore, D. A., and Erickson, H. P. (2013). The C-terminal linker of E Scherichia coli FtsZ functions as an intrinsically disordered peptide. *Mol. Microbiol.* 89, 264–275. doi: 10.1111/mmi.12279

Guan, F., Yu, J., Yu, J., Yang, L., Li, Y., Feng, X.-H., et al. (2018). Lateral interactions between Protofilaments of the bacterial tubulin homolog FtsZ are essential for cell division. *eLife* 7:e35578. doi: 10.7554/eLife.35578

Hayashi, M., Nishiyama, M., Kazayama, Y., Toyota, T., Harada, Y., and Takiguchi, K. (2016). Reversible morphological control of tubulin-encapsulating Giant liposomes by hydrostatic pressure. *Langmuir* 32, 3794–3802. doi: 10.1021/acs.langmuir.6b00799

Ishii, A., Nakasone, K., Sato, T., Wachi, M., Sugai, M., Nagai, K., et al. (2002). Isolation and characterization of the Dcw cluster from the Piezophilic Deep-Sea bacterium *Shewanella Violacea. J. Biochem.* 132, 183–188. doi: 10.1093/oxfordjournals.jbchem.a003208

Ishii, A., Sato, T., Wachi, M., Nagai, K., and Kato, C. (2004). Effects of high hydrostatic pressure on bacterial cytoskeleton FtsZ polymers in vivo and in vitro. *Microbiology* 150, 1965–1972. doi: 10.1099/mic.0.26962-0

Jaiswal, R., Patel, R. Y., Asthana, J., Jindal, B., Balaji, P. V., and Panda, D. (2010). E93R substitution of *Escherichia Coli* FtsZ induces bundling of Protofilaments, reduces GTPase activity, and impairs bacterial cytokinesis. *J. Biol. Chem.* 285, 31796–31805. doi: 10.1074/jbc.M110.138719

Jindal, B., and Panda, D. (2013). Understanding FtsZ assembly: cues from the behavior of its N-and C-terminal domains. *Biochemistry* 52, 7071–7081. doi: 10.1021/bi400129j

Kato, C., Li, L., Nogi, Y., Nakamura, Y., Tamaoka, J., and Horikoshi, K. (1998). Extremely barophilic Bacteria isolated from the Mariana trench, challenger deep, at a depth of 11, 000 meters. *Appl. Environ. Microbiol.* 64, 1510–1513. doi: 10.1128/AEM.64.4.1510-1513.1998

Kawamoto, J., Kurihara, T., Yamamoto, K., Nagayasu, M., Tani, Y., Mihara, H., et al. (2009). Eicosapentaenoic acid plays a beneficial role in membrane organization and cell division of a cold-adapted bacterium, *Shewanella Livingstonensis* Ac10. *J. Bacteriol.* 191, 632–640. doi: 10.1128/JB.00881-08

Kawamoto, J., Sato, T., Nakasone, K., Kato, C., Mihara, H., Esaki, N., et al. (2011). Favourable effects of Eicosapentaenoic acid on the late step of the cell division in a Piezophilic bacterium, *Shewanella Violacea* DSS12, at high-hydrostatic pressures: high-pressure adaptation of a Piezophile. *Environ. Microbiol.* 13, 2293–2298. doi: 10.1111/j.1462-2920.2011.02487.x

Kawarai, T., Wachi, M., Ogino, H., Furukawa, S., Suzuki, K., Ogihara, H., et al. (2004). SulA-independent Filamentation of *Escherichia Coli* during growth after release from high hydrostatic pressure treatment. *Appl. Microbiol. Biotechnol.* 64, 255–262. doi: 10.1007/s00253-003-1465-6

Li, L., Kato, C., Nogi, Y., and Horikoshi, K. (1998). Distribution of the pressure-regulated operons in Deep-Sea Bacteria. *FEMS Microbiol. Lett.* 159, 159–166. doi: 10.1111/j.1574-6968.1998.tb12855.x

Lu, C., Stricker, J., and Erickson, H. P. (2001). Site-specific mutations of FtsZ-effects on GTPase and in vitro assembly. *BMC Microbiol.* 1:7. doi: 10.1186/1471-2180-1-7

Lyu, Z., Coltharp, C., Yang, X., and Xiao, J. (2016). Influence of FtsZ GTPase activity and concentration on nanoscale Z-ring structure in vivo revealed by three-dimensional superresolution imaging. *Biopolymers* 105, 725–734. doi: 10.1002/bip.22895

Ma, X., and Margolin, W. (1999). Genetic and functional analyses of the conserved C-terminal core domain of *Escherichia Coli* FtsZ. *J. Bacteriol.* 181, 7531–7544. doi: 10.1128/JB.181.24.7531-7544.1999

Marteyn, B. S., Karimova, G., Fenton, A. K., Gazi, A. D., West, N., Touqui, L., et al. (2014). ZapE is a novel cell division protein interacting with FtsZ and modulating the Z-ring dynamics. *mBio* 5, e00022–e00014. doi: 10.1128/mBio.00022-14

McGarrity, J. T., and Armstrong, J. B. (1981). The effect of temperature and other growth conditions on the fatty acid composition of *Escherichia Coli. Can. J. Microbiol.* 27, 835–840. doi: 10.1139/m81-128

Messier, P. E., and Seguin, C. (1978). The effects of high hydrostatic pressure on microfilaments and microtubules in *Xenopus Laevis. J. Embryol. Exp. Morphol.* 44, 281–295.

Monahan, L. G., Robinson, A., and Harry, E. J. (2009). Lateral FtsZ association and the assembly of the Cytokinetic Z ring in Bacteria. *Mol. Microbiol.* 74, 1004–1017. doi: 10.1111/j.1365-2958.2009.06914.x

Monteiro, J. M., Pereira, A. R., Reichmann, N. T., Saraiva, B. M., Fernandes, P. B., Veiga, H., et al. (2018). Peptidoglycan synthesis drives an FtsZ-treadmilling-independent step of cytokinesis. *Nature* 554, 528–532. doi: 10.1038/nature25506

Moussa, M., Perrier-Cornet, J.-M., and Gervais, P. (2007). Damage in *Escherichia Coli* cells treated with a combination of high hydrostatic pressure and subzero temperature. *Appl. Environ. Microbiol.* 73, 6508–6518. doi: 10.1128/AEM.01212-07

Mukherjee, A. (1998). Dynamic assembly of FtsZ regulated by GTP hydrolysis. *EMBO J.* 17, 462–469. doi: 10.1093/emboj/17.2.462

Mukherjee, A., and Lutkenhaus, J. (1994). Guanine nucleotide-dependent assembly of FtsZ into filaments. *J. Bacteriol.* 176, 2754–2758. doi: 10.1128/jb.176.9.2754-2758.1994

Nishiyama, M. (2017). High-pressure microscopy for tracking dynamic properties of molecular machines. *Biophys. Chem.* 231, 71–78. doi: 10.1016/j.bpc.2017.03.010

Nishiyama, M., Shimoda, Y., Hasumi, M., Kimura, Y., and Terazima, M. (2010). Microtubule depolymerization at high pressure. *Ann. N. Y. Acad. Sci.* 1189, 86–90. doi: 10.1111/j.1749-6632.2009.05411.x

Okuno, D., Nishiyama, M., and Noji, H. (2013). Single-molecule analysis of the rotation of F1-ATPase under high hydrostatic pressure. *Biophys. J.* 105, 1635–1642. doi: 10.1016/j.bpj.2013.08.036

Perez, A. J., Cesbron, Y., Shaw, S. L., Villicana, J. B., Tsui, H.-C. T., Boersma, M. J., et al. (2019). Movement dynamics of Divisome proteins and PBP2x: FtsW in cells of *Streptococcus Pneumoniae. Proc. Natl. Acad. Sci. USA* 116, 3211–3220. doi: 10.1073/pnas.1816018116

Redick, S. D., Stricker, J., Briscoe, G., and Erickson, H. P. (2005). Mutants of FtsZ targeting the Protofilament Interface: effects on cell division and GTPase activity. *J. Bacteriol.* 187, 2727–2736. doi: 10.1128/JB.187.8.2727-2736.2005

Salmon, E. D. (1975a). Pressure-induced Depolymerization of brain microtubules in vitro. *Science (New York, N.Y.)* 189, 884–886. doi: 10.1126/science.1171523

Salmon, E. D. (1975b). Pressure-induced Depolymerization of spindle microtubules. I. Changes in birefringence and spindle length. *J. Cell Biol.* 65, 603–614. doi: 10.1083/jcb.65.3.603

Schindelin, J., Arganda-Carreras, I., Frise, E., Kaynig, V., Longair, M., Pietzsch, T., et al. (2012). Fiji: an open-source platform for biological-image analysis. *Nat. Methods* 9, 676–682. doi: 10.1038/nmeth.2019

Schumacher, M. A., Huang, K.-H., Zeng, W., and Janakiraman, A. (2017). Structure of the Z ring-associated protein, ZapD, bound to the C-terminal domain of the tubulin-like protein, FtsZ, suggests mechanism of Z ring stabilization through FtsZ cross-linking. *J. Biol. Chem.* 292, 3740–3750. doi: 10.1074/jbc.M116.773192

Schumacher, M. A., Zeng, W., Huang, K.-H., Tchorzewski, L., and Janakiraman, A. (2016). Structural and functional analyses reveal insights into the molecular properties of the *Escherichia Coli* Z ring stabilizing protein, ZapC. *J. Biol. Chem.* 291, 2485–2498. doi: 10.1074/jbc.M115.697037

Shin, J. Y., Vollmer, W., Lagos, R., and Monasterio, O. (2013). Glutamate 83 and arginine 85 of Helix H3 bend are key residues for FtsZ polymerization, GTPase activity and cellular viability of *Escherichia Coli*: lateral mutations affect FtsZ polymerization and *E. coli* viability. *BMC Microbiol.* 13:26. doi: 10.1186/1471-2180-13-26

Siebenaller, J. F. (2003). Pressure effects on the GTPase activity of brain membrane G proteins of deep-living marine fishes. *Comp. Biochem. Physiol. B: Biochem. Mol. Biol.* 135, 697–705. doi: 10.1016/S1096-4959(03)00165-9

Siebenaller, J. F., and Murray, T. F. (1994). The effects of hydrostatic pressure on the low-K m GTPase in brain membranes from two congeneric marine fishes. *J. Comp. Physiol. B.* 163, 626–632. doi: 10.1007/BF00369512

Stricker, J., and Erickson, H. P. (2003). In vivo characterization of *Escherichia Coli* ftsZ mutants: effects on Z-ring structure and function. *J. Bacteriol.* 185, 4796–4805. doi: 10.1128/JB.185.16.4796-4805.2003

Stricker, J., Maddox, P., Salmon, E. D., and Erickson, H. P. (2002). Rapid assembly dynamics of the *Escherichia Coli* FtsZ-ring demonstrated by fluorescence recovery after photobleaching. *Proc. Natl. Acad. Sci.* 99, 3171–3175. doi: 10.1073/pnas.052595099

Sundararajan, K., and Goley, E. D. (2017). The intrinsically disordered C-terminal linker of FtsZ regulates Protofilament dynamics and superstructure in vitro. *J. Biol. Chem.* 292, 20509–20527. doi: 10.1074/jbc.M117.809939

Szwedziak, P., Wang, Q., Bharat, T. A. M., Tsim, M., and Löwe, J. (2014). Architecture of the ring formed by the tubulin homologue FtsZ in bacterial cell division. *eLife* 3:e04601. doi: 10.7554/eLife.04601

Takiguchi, K., Hayashi, M., Kazayama, Y., Toyota, T., Harada, Y., and Nishiyama, M. (2018). Morphological control of microtubule-encapsulating Giant vesicles by changing hydrostatic pressure. *Biol. Pharm. Bull.* 41, 288–293. doi: 10.1248/bpb.b17-00366

Tamby, A., Sinninghe Damsté, J. S., and Villanueva, L. (2023). Microbial membrane lipid adaptations to high hydrostatic pressure in the marine environment. *Front. Mol. Biosci.* 9:1058381. doi: 10.3389/fmolb.2022.1058381

Wagstaff, J. M., Tsim, M., Oliva, M. A., García-Sanchez, A., Kureisaite-Ciziene, D., Andreu, J. M., et al. (2017). A polymerization-associated structural switch in FtsZ that enables Treadmilling of model filaments. *mBio* 8, e00254–e00217. doi: 10.1128/mBio.00254-17

Welch, T. J., and Bartlett, D. H. (1998). Identification of a regulatory protein required for pressure-responsive gene expression in the deep-sea bacterium Photobacterium species strain SS9. *Mol. Microbiol.* 27, 977–985. doi: 10.1046/j.1365-2958.1998.00742.x

Xiao, X., Zhang, Y., and Wang, F. (2021). Hydrostatic pressure is the universal key driver of microbial evolution in the deep ocean and beyond. *Environ. Microbiol. Rep.* 13, 68–72. doi: 10.1111/1758-2229.12915

Yang, X., Lyu, Z., Miguel, A., McQuillen, R., Huang, K. C., and Xiao, J. (2017). GTPase activity–coupled treadmilling of the bacterial tubulin FtsZ organizes septal cell wall synthesis. *Science* 355, 744–747. doi: 10.1126/science.aak9995

Yin, Q.-J., Zhang, W.-J., Qi, X.-Q., Zhang, S.-D., Jiang, T., Li, X.-G., et al. (2017). High hydrostatic pressure inducible trimethylamine N-oxide reductase improves the pressure tolerance of piezosensitive bacteria *Vibrio Fluvialis. Front. Microbiol.* 8:2646. doi: 10.3389/fmicb.2017.02646